Materials Science Forum Vol. 792 (2014) pp 379-384

doi:10.4028/www.scientific.net/MSF.792.379

Investigation of magnet arrangements in Double Layer Interior Synchronous Permanent Magnet Motor over wide-speed range for Electric Vehicle applications

Athanasios G. Sarigiannidis[1,a], Minos E. Beniakar[1], Panagiotis E. Kakosimos[1] and Antonios G. Kladas[1]

[1] School of Electrical and Computer Engineering, National Technical University of Athens, GR-15780, Athens, Greece

[a]thsarig@central.ntua.gr

Keywords: Interior Synchronous Permanent Magnet Motors, field weakening capability, Maximum Torque per Ampere control, magnetic saturation, finite elements, electric vehicle applications.

Abstract. In this paper, the magnet arrangement for a manufactured Double Layer Interior Synchronous Permanent Magnet Motor (DLISPMM) for Electric Vehicle (EV) applications is investigated. In a first step, the manufactured motor is optimized for its nominal condition, by using a particular design of experiment (DOE) method. In a second step, a comparative analysis for the two types of DLISPMMs for a wide speed range operation is performed, by using a parametric Finite Element (FE) model, for calculation of the main machine characteristics, in conjunction with a convenient dynamic model, considering magnetic saturation, for implementation of field weakening control. The initial linear and the final, considering magnetic saturation, dynamic models are evaluated. Finally, the initial and final designs are compared in terms of the main operating characteristics for both nominal low speed and high speed field weakening operation.

Introduction

The Interior Permanent Synchronous Magnet Motors (IPSMMs) are considered to be an advantageous option for EV applications, due to their superior nominal characteristics, including high efficiency, torque density and a wide speed operating range, with the adequate magnet shielding, issues of crucial importance in EV applications [1,3]. In IPMM with single layer (SL) permanent magnet, the saliency in magnetic circuit, as illustrated in figure 1a creates a discrepancy in *d* and *q* axis inductances, resulting in a reluctance torque, additional to the magnet torque produced by the permanent magnets. In order to enhance the saliency of the magnetic circuit and extend the speed range, DLISPMM configurations are adopted [1]. Generally speaking, there are several topologies for DLISPMM [2]. In this paper, the 2I and VI topologies, as illustrated in Fig. 1b and 1c, respectively, will be analyzed, over wide speed range. The DLISPMM for EV applications manufactured by Brusa Electronik, is a 2I topology [1], with its main dimensional and operational characteristics, taken by a FE analysis, tabulated in table 1.

Table 1. Initial DLISPMM configuration

Main Dimensional Characteristics		Nominal Operational Characteristics	
Phases, Poles, Slots	3, 6, 54	P=Power [kW], n=Speed [rpm]	16.5, 2000
R_{so}=Diameter of stator [cm]	24	J=Current density [A/mm^2]	4.5
L=core length [cm]	12.3	T_e, T_{ripple}=Mean Torque [Nm], Torque ripple (%)	78.9, 35.9
l_{1mag}, l_{2mag} =1st, 2nd layer magnet length [mm]	39 , 21	EMF_{rms}=Induced back electromagnetic force [V]	76.3
w_{1mag}, w_{2mag}=1st, 2nd layer magnet width [mm]	7.8, 4	Φ_{mag}=Flux linkage induced by magnets [Wb]	0.1205
D_s=Slot depth, T_w=Tooth width [mm]	20.9, 5.4	$P_{FE,}$ P_{cu}=Iron, Copper losses [W], η=efficiency (%)	153, 846, 94.81

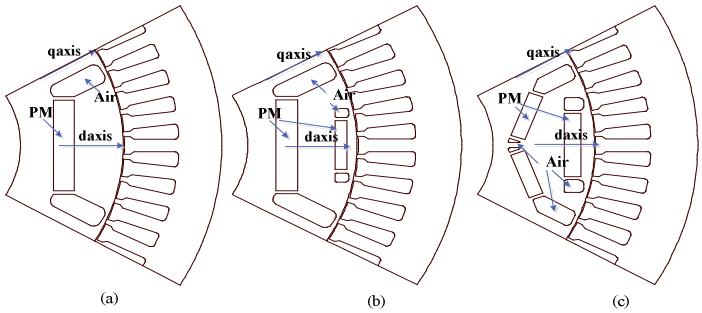

Fig.1 IPMM Topologies: (a) SL (b) DL-2I (c) DL-VI

Design of Experiment (DOE) Optimization procedure

In this application, the DOE optimization technique has been implemented, because of the small domain of the design variables and the close distance from the global optimum, rendering the DOE optimization algorithm a favourable option. The optimization procedure is illustrated in Fig. 2. The X_i and Y_i variables are assigned as $X_i=[w_{1mag}\ w_{2mag}]$ with $l_{2mag}=f(X_i)$ so as to keep the total volume of the magnet constant and $Y_i=[\theta_{mag}]$. It is worthwhile to be mentioned that the optimization procedure has been executed for the nominal operation (n=2000rpm, J=4.5A/mm^2). Initially, the optimization procedure starts with the initial design variables of 2I topology, as shown in table 1. In a second step, the DOE optimization algorithm searches the X_i variables that minimize the objective function for the 2I topology. After finding the motor geometry that minimizes the objective function for the 2I topology, the DOE optimization algorithm implements the same procedure with the Y_i design variable for the VI topology. It should be noted that the objective function is mainly focused to reduce the torque ripple and the harmonic content of the EMF, in conjunction with retaining the mean torque around the nominal value, in a range of ±2%, which is a constraint of the optimization process. The objective function is expressed as follows:

$$F=\frac{T_{ripple}}{T_{rippleinit}}+\frac{EMF_{THD}}{EMF_{THDinit}} \tag{1}$$

where F is the objective function, T_{ripple}, $T_{rippleinit}$ are the measured torque ripple for each design variable and for the initial geometry, respectively and EMF_{THD}, $EMF_{THDinit}$ are the Total Harmonic Distortion of the induced back EMF for each design variable and for the initial geometry, respectively. The proposed final geometry is of VI topology, with w_{1mag}=5.1mm, w_{2mag}=6.7mm, l_{1mag}=39mm, l_{2mag}=27.1973mm, θ_{mag}=139.2 degrees. From the proposed permanent magnets (PM) dimensions it can be observed that the outer layer of PMs has approximately the same magnet volume with the inner PM layer, in contrast with the initial PMs configuration.

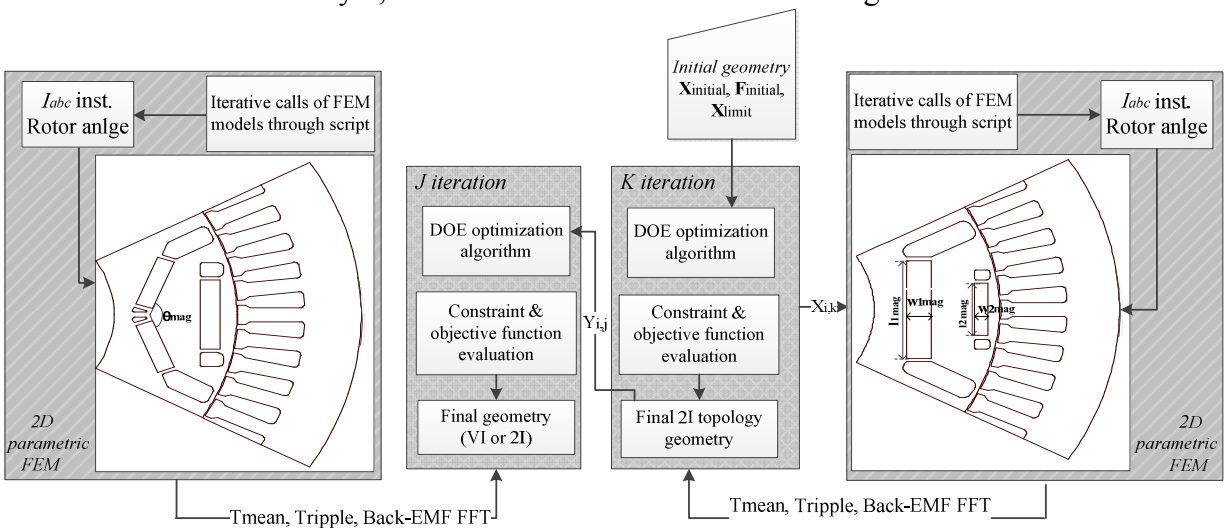

Fig.2 Optimization algorithm overview

Double Layer Interior Synchronous Permanent Magnet Motor control technique

The DLISPMM operates on two main operating regions, the constant torque region for low speed and the constant power-field weakening region for high speed region, because of the specifications of EV applications. In EV applications, a high torque capability motor with high speed operating range is required, because of the constant transmission ratio of the gearbox and the high required range in EV velocity, as the vehicle is driven in urban or rural environment [6]. Furthermore, field weakening capability is required in order to keep the stator voltage to a specific level, which is usually low in EV applications, mainly for safety reasons. The required torque-speed curve for the investigated DLISPMM is shown in Fig. 3.

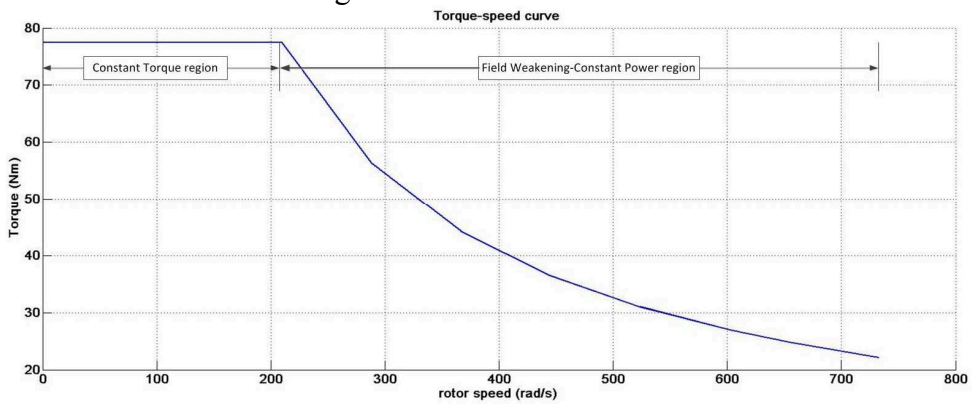

Fig.3 Torque-speed curve of DLISPMM

Initially, in order to design the dynamic control model for the DLISPMM, the motor has been analyzed in *q-d* reference frame. The *d* and *q*-axis currents, fluxes, and voltages of the DLISPMM are expressed in q-d reference frame as follows:

$$I_d = -I_a \bullet \sin\beta \tag{2}$$

$$I_q = I_a \bullet \cos\beta \tag{3}$$

$$\Phi_d = L_d \bullet I_d + \Phi_{mag} \tag{4}$$

$$\Phi_q = L_q \bullet I_q \tag{5}$$

$$V_d = R_a \cdot I_d - \omega \cdot \Phi_q = R_a \cdot I_d - \omega \cdot L_q \cdot I_q \tag{6}$$

$$V_q = R_a \cdot I_q + \omega \cdot \Phi_d = R_a \cdot I_q + \omega \cdot L_d \cdot I_d + \omega \cdot \Phi_{mag} \tag{7}$$

$$V_a = \sqrt{V_q^{\,2} + V_d^{\,2}} \le \frac{V_{DC}}{\sqrt{2}} \tag{8}$$

where I_d and I_q are the *d* and *q*-axis currents, Φ_d and Φ_q are the *d* and *q*-axis fluxes, L_d and L_q are the *d* and *q*-axis inductances, V_d and V_q are the *d* and *q*-axis voltages, respectively, R_a is the armature resistance, ω is the angular frequency, V_a and V_{DC} are the armature AC voltage and the inverter DC voltage, respectively. By using these values, the torque T_e is expressed as follows:

$$T_e = \frac{3}{2} p \cdot \left(\Phi_{mag} \cdot I_q + \left(L_d - L_q \right) \cdot I_d \cdot I_q \right) \tag{9}$$

where $3/2p\Phi_{mag}I_q$ is the magnet torque, whereas $3/2p(L_d\text{-}L_q)I_dI_q$ is the reluctance torque. This expression is widely used to understand the torque characteristics of the interior permanent magnet motors. Strictly speaking, not only L_d and L_q, but also Φ_{mag} vary with load conditions because of the magnetic saturation in the core. In this study, L_d and L_q are assumed to be functions of the armature current, taken from the FE analysis, whereas the Φ_{mag} is assumed to be constant for simplicity.

For constant torque region the Maximum Torque per Ampere (MTPA) method is evaluated [4]. MTPA can be achieved by differentiating Eq. 9 with respect to *q*-axis current I_q and set it to zero which gives:

$$I_d = \frac{\Phi_{mag}}{2 \cdot \left(L_q - L_d \right)} - \sqrt{\frac{\Phi_{mag}^2}{4 \cdot \left(L_q - L_d \right)^2} + I_q^2} \tag{10}$$

Substituting equation (10) to (9) one can get the nonlinear relation between I_q and T_e, which is:

$$T_e = \frac{3p}{2}\bullet\left(\Phi_{mag}\cdot I_q - \frac{\Phi_{mag}\cdot I_q}{2} - \left(L_d - L_q\right)\bullet\sqrt{\frac{\Phi_{mag}^2\cdot I_q^2}{4\cdot\left(L_q - L_d\right)^2} + I_q^4}\right) \tag{11}$$

An overview of the field oriented control for wide speed range operations, based on the *q-d* equations for the DLISPMM (Eq.2-9), accounting for magnetic saturation, (L_d, L_q=*f(I)*), the required torque-speed curve as shown in Fig. 3 and the MTPA functions, as shown in Eq.10,11 for constant torque region is illustrated in Fig. 4, respectively. The function L_d, L_q=*f(I)* has been taken from the FE analysis and it is shown in Fig. 8. In addition, a particular flux weakening constant has been introduced, in order to increase the demagnetizing I_d current, while decreasing the active I_q current, in order to lower the electromagnetic torque. The value of this constant is one for the constant torque region and in constant power region it decreases as depicted in Fig. 4. Moreover, a hysteresis current regulator has been chosen as modulation technique for the voltage fed inverter, as it is regarded a suitable and stable selection for medium power synchronous motors [5].

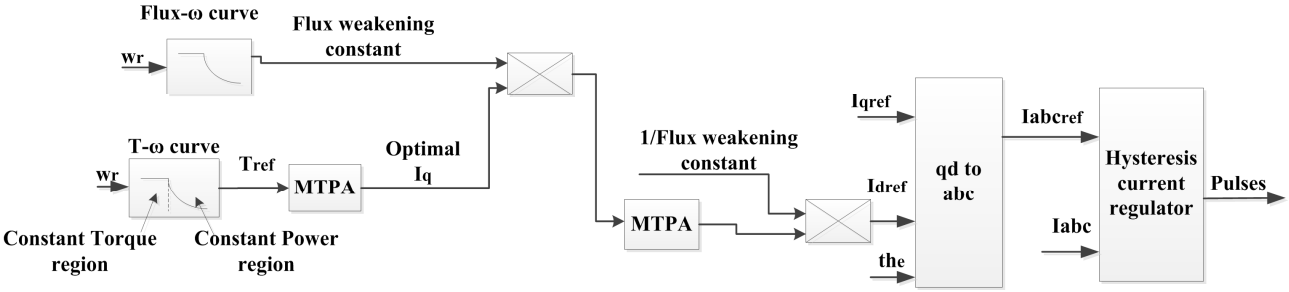

Fig.4 DLISPMM control technique overview

In a second step, the control model presented above has been simulated for a mechanical load T_L/ω=0.042 Nm/(rad/s), system moment of inertia J=0.02 kg.m^2 and dc input voltage V_{dc}=270V, in order to investigate the transient behavior of the DLISPMM. The reference and simulated torque versus time and the speed response for the initial design are illustrated in Fig. 5a and 5b, respectively. From Fig. 5a, it can be observed that the control reacts adequately, as the measured electromagnetic torque follows the reference torque. The peak values of stator voltages (V,V_d,V_q) and machine currents (I,I_q,I_d), for the linear and considering magnetic saturation models are depicted in Fig. 6 and 7, respectively. From Fig. 6 and 7 it is evident that the model considering the variation of *d* and *q* axis inductances requires a higher stator voltage, in order to produce the same electromagnetic torque, thanks to the higher L_d,L_q for lower current, which should be considered for the adequate voltage level of the dc bus of the inverter, in order to drive the DLISPMM for high speeds. Furthermore, from Fig.6 and 7 the field weakening operation after n=2000 rpm can be observed, where the absolute value of d-axis current I_d is increased, while the q-axis current I_q is decreased, in order to keep the EMF constant to a reference value.

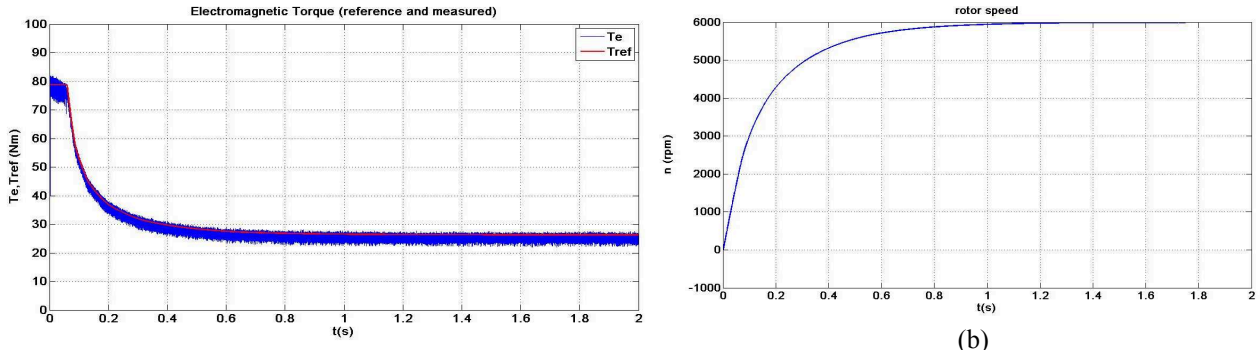

(a) (b)

Fig. 5 Reference, measured electromagnetic torque (a) and rotor speed (b) of DLISPMM versus time

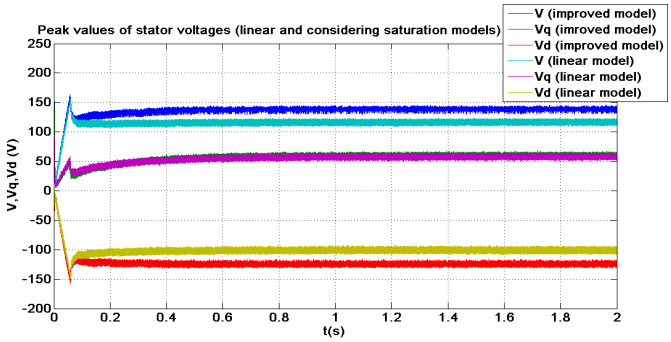

Fig. 6 Peak values of DLISPMM stator voltages versus time for linear and considering magnetic saturation models

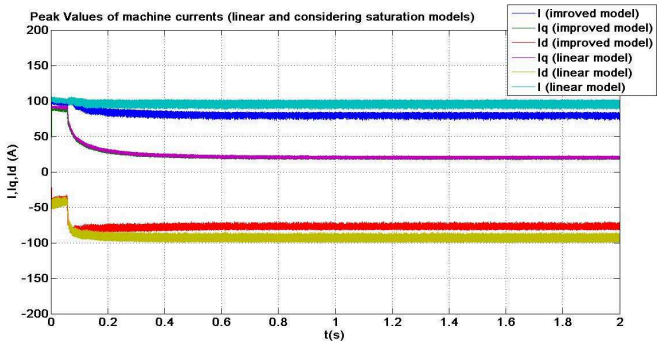

Fig. 7 Peak values of DLISPMM line currents versus time for linear and considering magnetic saturation models

Results and discussion

The initial and final geometry have been analyzed via the parametric time stepping FEM model at nominal operation (n=2000prm) and at high speed state (n=6000rpm), considering the torque and the d-q axis machine currents, taken from the transient control model analyzed above, for the field weakening implementation. Initially, the variation d,q axis inductances has been calculated by the FE analysis, in order to be introduced in the transient control model and is shown in Fig. 8.

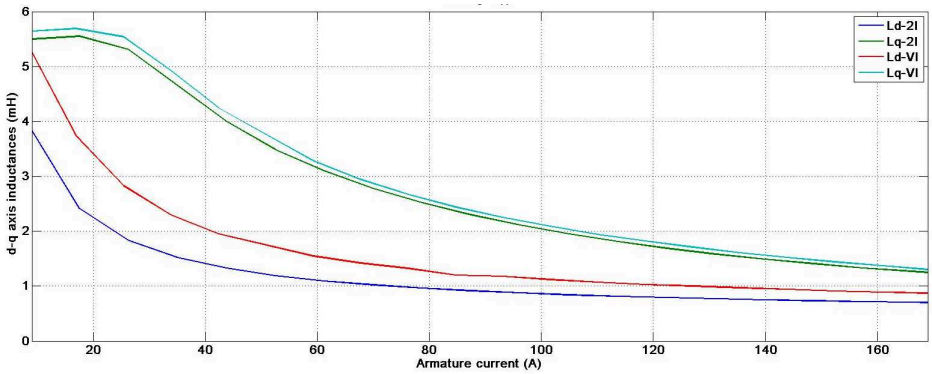

Fig. 8. D and q axis inductances for the initial and final proposed design versus armature current

Table 2 summarizes the results obtained from the field FE analysis for nominal and field weakening operation. From table 2 it can be concluded that the proposed topology has quite lower torque ripple at nominal state, which is extremely important due to the high value of the torque ripple of the initial geometry. Furthermore, it can be observed that the other characteristics remain approximately the same. On the other hand, based on the simulated results, it can be concluded that the VI topology operates more satisfactory than 2I topology, under field weakening region, as the flux leakage from permanent magnets is lower, so lower absolute I_d is needed to weaken the field, in order to retain the stator voltage to the appropriate value. Furthermore, because of the iron bridge created between the inside magnets in the VI topology, which increases the leakage of the magnet flux, the rest part of iron in stator and rotor is less saturated than in 2I topology, which results in less iron losses, which can be validated by the simulation. Moreover, the magnetic field distribution at

nominal state for both DLISPMM topologies is depicted in Fig.9. From Fig.9, significant magnetic saturation can be observed at teeth, along *q* axis iron and iron bridges.

Table 2. Main characteristics of the initial and proposed topology under two operating conditions

Topology	Nominal operation (n=2000rpm)		Field weakening operation (n=6000rpm)	
	2I	VI	2I	VI
T_e [Nm], T_{ripple} (%)	78.9 , 35.9	78.04, 25.6	22.7, 63.4	23.8, 45.8
$EMF_{Fund.}$ [V], THD (%)	76.3, 15.17	79.9, 16.4	119.2, 39.85	111.6, 54.3
J [A/mm^2], Φ_{mag} [Wb]	4.5, 0.1205	4.5, 0.0965	3.71, 0.1205	3.55, 0.0965
P_{cu}, P_{FE} [W], η (%)	846 , 153, 94.81	846 , 132, 94.35	575.1 , 599.9, 92.38	511.4 , 412.1 , 94.18

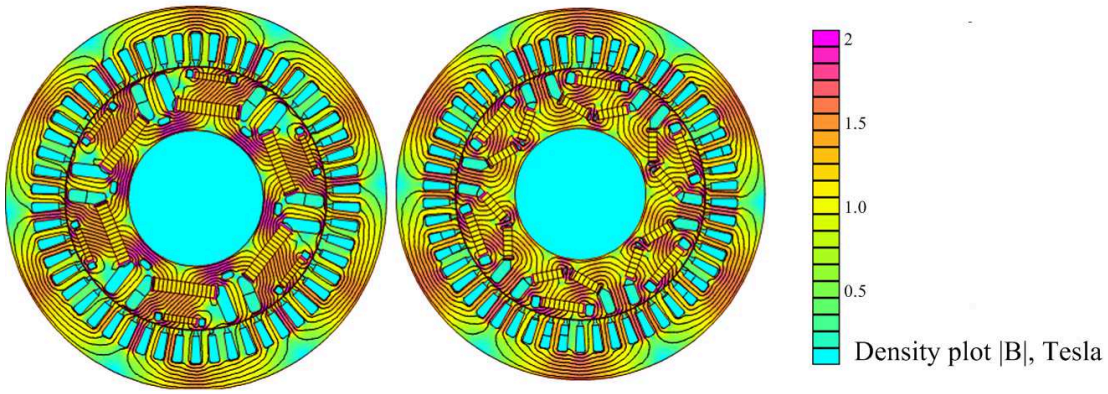

Fig.9 Magnetic field density distribution for nominal load of the initial and the proposed DLISPMMs

Summary

In this paper, the most suitable PM topology for DLISPMM for EV applications has been examined. The analysis has been implemented by both using FE and transient field oriented control models, in order to evaluate the optimized PM topology to more than one operating conditions. From the analysis made, it has been validated that the optimized VI topology has superior operating characteristics, in terms of efficiency and torque ripple, particularly in high speed field weakening operation, due to the higher leakage magnet flux created by the PM topology.

Acknowledgement

Mr. Athanasios Sarigiannidis is supported in his PhD studies by "IKY Fellowships of Excellence for Postgraduate Studies in Greece - Siemens Program". Additionally, part of this research has been co-financed by the European Union (European Social Fund - ESF) and Greek national funds under the General Secretariat for Research and Technology of Greece, Program: 09ΣΥΝ-51-1015 Technology assessment for hybrid and electric vehicles application in the greek environment".

References

[1] A. Muntean et al., "Torque Analysis and Control of Double Layer Interior Synchronous Permanent Magnet Motor for Electric Vehicle Propulsion Applications," *Electromotion*, 2009.

[2] K. Yamazaki, K. Kitayuguchi, "Investigation of Magnet Arrangements in Double Layer Interior Permanent Magnet Motor," *ECCE*, 2010.

[3] P. E. Kakosimos, A. G. Sarigiannidis, M. E. Beniakar, A.G. Kladas, and C. Gerada, "Induction Motors versus Permanent Magnet Actuators for Aerospace Applications," *IEEE Trans. Ind. Electron.*, vol.61, no.9, pp. 4315-4325, Aug. 2014.

[4] M. A. Hoque, C. Butt and M. A. Rahman, "A Novel Approach for MTPA Speed Control of IPMSM Drive," *2nd International Conference on Electrical and Computer Engineering*, 2002.

[5] Lazi J. M. et al., "Performance comparison of SVPWM and Hysteresis Current Control for Dual motor drives," *Applied Power Electronics Colloquium (IAPEC)*, 2011.

[6] Larminie J., Lowry J., "Electric Vehicle Technology Explained," *John Wiley and Sons*, 2003.